ACTA NEUROBIOLOGIAE EXPERIMENTALIS

Acta Neurobiol. Exp. 2003, 63: 83-98

Rate coding: neurobiological network performing detection of the difference between mean spiking rates

Juraj Pavlásek[1], **Ján Jenča**[1] and **Radoslav Harman**[2]

[1]Department of Neurophysiology, Institute of Normal and Pathological Physiology, Slovak Academy of Sciences, 1 Sienkiewicz St., 81371 Bratislava 1, Slovakia; [2]Department of Theoretical Probability and Mathematical Statistics, Faculty of Mathematics, Physics and Informatics, Comenius University, Mlynská Dolina, 84248 Bratislava 4, Slovakia

Abstract. We propose a network of model neurones that "reads" the information encoded as a mean spiking rate by mechanisms relevant to the organism. The streams of independent irregular spiking activity with a Poisson distribution enters the network in parallel *via* two inputs. The network integrates both synaptic inputs and at the same time acts as a counter allowing their continuous comparison. Detection of the mean spiking rate difference is signalled by spikes emitted at the output. The exactness of the mean-rate discrimination was quantified by the probability of theoretically best comparison.

The corresondence should be addressed to J. Pavlasek, Email: unpfpavl@savba.sk

Key words: rate coding, model network, parallel channels, irregular spiking activity, discrimination, decoding

INTRODUCTION

A neural image of an adequate stimulus is represented by analogue nonlinearities (e.g., receptor potentials, synaptic potentials) and trains of the nerve action potentials (spikes) conveyed between neural cells. The number and timing of spikes produced by arrays of peripheral receptors and ensembles of activated neurones should encode each event (a stimulus) with sufficient resolution and accuracy to be distinguishable from other events.

There are two basic concepts concerning information transmission by strings of spikes in the domain of time coding. A rate code (the mean firing frequency) and an interspike interval code (the information is carried not simply by the array of intervals but by their sequence) (Pavlásek and Jenča 2001, Perkel and Bullock 1968, Rieke et al. 1999).

The rate-encoding hypotheses assume that the stimuli are encoded by setting the firing rate proportional to the values of some of their parameters. The information "read" by a postsynaptic neurone is correlated only with the number of elicited spikes (increase, decrease) within the encoding time window (Abbot and Sejnowski 1999, Nádasdy 2000, Theunissen and Miller 1995).

Adrian and Zotterman (1926) first noted the relationship between neuronal firing rate and stimulus intensity that forms the basis of rate coding. Further experimental work confirmed the rate code as an information processing strategy in several sensory systems - somatosensory (Hsiao et al. 1993, Mountcastle 1957), auditory (Konishi 1991) and visual (Girman et al. 1999, Towee et al.1993).

It is reasonable to suppose that in some modes of information processing the distinction between irregular spiking rates in two (or more) impulse-carrying pathways is of central importance. Neural mechanisms performing this task bring information about sensory magnitudes (which of two weights is heavier, or which of two lights is brighter) and about their changes (novelty detection). Therefore they could be involved in a decision-making (Platt and Glimcher 1999) and in adequate behavioural acts.

The lower firing rate imposes a serious problem for the rate encoder concept (Nádasdy 2000). The decisive parameter is the rate at which the neurone "forgets" its previous input. If the integration time is shorter than the intervals between successive input spikes, the neurone cannot "remember" its "history". Taking a value of 4.1-11.49 ms for the time constant of final decay of the excitatory postsynaptic potential into account (Redman and Walmsley 1983, Xu and Pulsinelli 1996), we should assume that in all neurones which fire at rates of 25 Hz or lower, the rate coding cannot be the method of information transmission (König et al. 1996). In this context it is interesting to note the experimental results which indicate that the lower firing rates are used in the CNS for information transmission as well (Willis and Coggeshall 1991).

In this article, we concentrate on proposing a small network that can carry out the decision-making function by continual comparison of the irregular spiking activities (mean rate 20 - 50 spikes/s) in two parallel channels. It is a conceptual solution based on an abstract network with operational principles widely used in the central nervous system.

METHODS

The computer model JASTAP obeys the principles concerning the physiology of a biologically realistic neurone with a chemical transmission of information. Details of the model have been reported elsewhere (Jančo et al. 1994). Here only a brief account is given of the essential properties used in the simulations shown in this paper.

The basic element of the network is a model neurone (neuroid) behaving as an integrate-and-fire element. It is described by:

1) Instantaneous membrane potential (MP). MP is a dimensionless quantity within the range [-1, 1] which is determined as the sum of postsynaptic potentials (PSP) limited by the non-linear function

$$MP(t) = (2/\pi)*\mathrm{arctg}(\Sigma PSP(t)) \quad (1)$$

2) The threshold (TH) is from the interval [0, 1]. In simulation experiments the TH was set constant (close to 0.5 for all neuroids).

3) The frequency of spikes (SP) is restricted by the absolute refractory period. Setting the maximum (Imx) and minimum (Imn) interspike intervals ensures this principle. The actual interspike interval (Ia) is determined as

$$Ia=Imx - (Imx - Imn)*(2/\pi)*\mathrm{arctg}((MP-TH)/(1-MP)) \quad (2)$$

The standard value for Imn was 1 ms, and Imx ranged from 2 ms to 10 ms.

Each neuroid can have 8 synaptic inputs but only a single output. The program treats the synapse as a part of

the neuroid. The output can be connected to one or several synapses in the network of neuroids.

A synapse is characterised by:

a) The input connected to it

b) The shape of a PSP prototype evoked by the SP arriving at this synapse (the particular waveform is selected from a set of prototype PSP shapes stored in a buffer of PSP waveforms). The PSP prototype (PSP_0) is described by

$$PSP_0(t) = k * \exp(-2*t/t2) * (1-\exp(-t/t1))^2 \qquad (3)$$

The waveform simulates whether the synapse in question is located on the soma or on the dendritic tree (the time-course and the attenuation of its amplitude). Experimental data were simulated with the parameters t1 = 1.6 and t2 = 6.4 ms.

c) The latency (time delay) of the synaptic transmission and/or axonal conduction.

d) The synaptic weight (SW) with its value from the interval [-1, 1]. SW simulates the effectiveness of a synaptic input (a synchronously activated set of axons of the same type or a cluster of the terminal branches of an axon). EPSPs were produced with the SW values from the interval [0, 1], IPSPs were produced with the SW values from the interval [-1, 0]. The value of the actual synaptic weight, and the PSP prototype determines the postsynaptic potential:

$$PSP(t) = SW * PSP_0(t) \qquad (4)$$

e) The event-dependent (plastic) changes which determine instantaneous, effective SW.

The computer program JASTAP has been written in C++ language. The program can define a network by simple command language and simulate its activity in discrete time intervals (0.5 ms steps). Samples of simulated activity can be displayed in the form of an intracellular recording with a microelectrode, or as a raster map of the spike potentials.

RESULTS

Processing of the rate-encoded information: Synaptic integration with a reasonable dynamic range

The rate-encoded information arrives at a sensory neurone *via* a plethora of synaptic endings. A "high input regime" of irregular excitatory signals might produce a "saturation" of the summation capacity of the integrate-and-fire device. Resulting sustained regular spiking (deCharms and Zador 2000, Segundo et al. 1968) deteriorates the dynamic range of the sensory neurone and prevents it from ability to distinguish the input stimuli. An integrate-and-fire neurone that balances excitation and inhibition produces irregular interspike intervals (ISI) (Shadlen and Newsome 1994). The variation in ISI is an unavoidable precondition for an effective discrimination of the spiking rates.

We modified the excitation of the integration neuroid (Fig. 1A, neuroid 0) by a "local" mechanism represented by a recurrent inhibition (Fig. 1A, neuroid 1). Each single spike in any of the three excitatory inputs (Fig. 1A, i0, i1 and i2) depolarised the neuroid 0 by 73% of the threshold (Fig. 1B, neuroid 0, i0, i1 and i2). If two or more spikes arrived within a 4.5 ms interval the neuroid 0 emitted a spike (SP). Each SP of the neuroid 0 activated the inhibitory feedback (Fig. 1A, neuroid 1) that produced a hyperpolarization of the neuroid 0 amounting to 21% of the resting membrane potential. The depolarising - hyperpolarizing shifts of the membrane potential lasted for about 25 ms (Fig. 1B, neuroid 0, i0+i1+i2).

A well-known theorem in stochastic point processes (Cox and Smith 1954) states that the independent channels conveying impulses, give rise, when pooled, to a sequence of impulses that closely resembles a Poisson process. An ideal homogeneous Poisson process simulated the pulse train in each of three inputs to the integration neuroid (Fig. 2A, i0, i1 and i2). It stands to reason that a spike train in a single input cannot be exact Poisson processes because the spikes cannot come too close together (considering the refractory period after an action potential). But it is a quantifiable random process suitable for testing the neuroid's ability to integrate an irregular afferentation (Fig. 2A, neuroid 0). The equation $\lambda=1/\overline{IPI}$ expresses the intensity of the Poisson process, where $\overline{IPI}$ is the expected (mean) value of the interpulse intervals. That is, the intervals T_i between subsequent pulses form a sequence of independent random variables distributed according to the exponential distribution Exp (λ):

$$P[T_i < t] = 1-\exp(-\lambda*t),\ t>0 \qquad (5)$$

For an irregular pulse signalling the resulting variation of intervals can be quantified by the coefficient of variation (CV = standard deviation/mean). In the case of the random input (i.e., a synthetic Poisson), CV for IPI

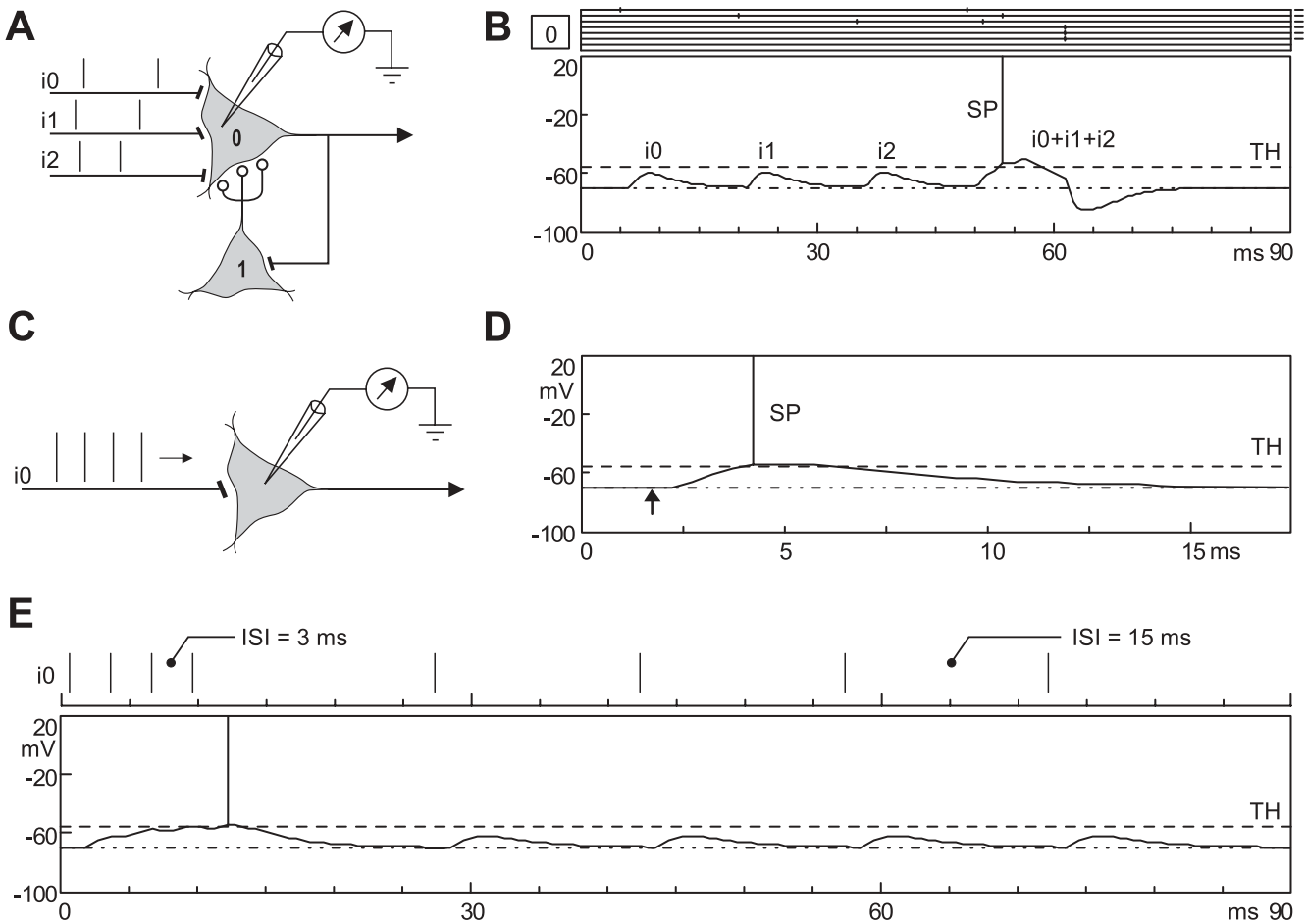

Fig. 1. The spatio-temporal summation of the simulated postsynaptic potentials. A, multiple excitatory inputs modified by a recurrent inhibition. Connections marked by bars (circles) are excitatory (inhibitory); B, simulated postsynaptic potentials (PSPs) in neuroid 0 evoked by a spiking activity in parallel inputs (i0, i1 and i2). Eight horizontal lines above the recordings represent possible synaptic inputs. The small vertical bars superimposed on them indicate spikes arriving at the synaptic endings (the active inputs are marked by short horizontal lines on the right hand side). The dashed horizontal line is the threshold (TH) level for spike (SP) generation (a vertical bar on the simulated recordings). The lower (dash-dot-dot) horizontal line represents resting transmembrane potential. A synaptic weight (SW) of i0, i1 and i2 was of subthreshold intensity (SW i0 = i1 = i2 = 0.6 TH). Two or a cluster of more SPs arriving at the synaptic endings in a short sequence (i0+i1+i2) evoked SP in the neuroid 0 and consequently in the inhibitory neuroid 1. The excitatory and inhibitory influences were integrated in depolarizing - hyperpolarizing shifts of the neuroid 0 membrane potential. Abscissa - simulation time in ms, ordinate - simulation of the transmembrane potential in mV providing approximate PSP amplitude range in a biologically realistic neurone; C, a neuroid excited by regular spiking activity arriving along a single channel (i0); D, the time-course of the simulated excitatory postsynaptic potential (EPSP) evoked by a single spike arriving at the synaptic ending (an arrow) with a suprathreshold synaptic strength (SW = 1.02 TH); E, different modes of a subthreshold (SW = 0.5 TH) excitatory drive of the neuroid with an EPSP time-course illustrated in D. In upper part is a raster display of the input spikes (i0). The first group of four spikes with an interspike interval (ISI) = 3 ms (333 Hz), the second group of four spikes with ISI = 15 ms (66 Hz). Only the EPSPs evoked by the first group of spikes summed up and exceeded the spike-threshold level.

distribution (CV_{IPI}) equals to 1. We will refer to the CV of the interspike interval (ISI) distribution (CV_{ISI}) when evaluating the dynamic range of the efferent spiking of the integrating unit (Fig. 2A, neuroid 0).

The input trains with three different intensities ($\overline{IPI}$ = 19, 32 and 52.5 ms) (Fig. 2B) were used for simulation experiments. In individual simulations the intensities of all Poisson processes were the same (Fig. 2A, i0, i1 and

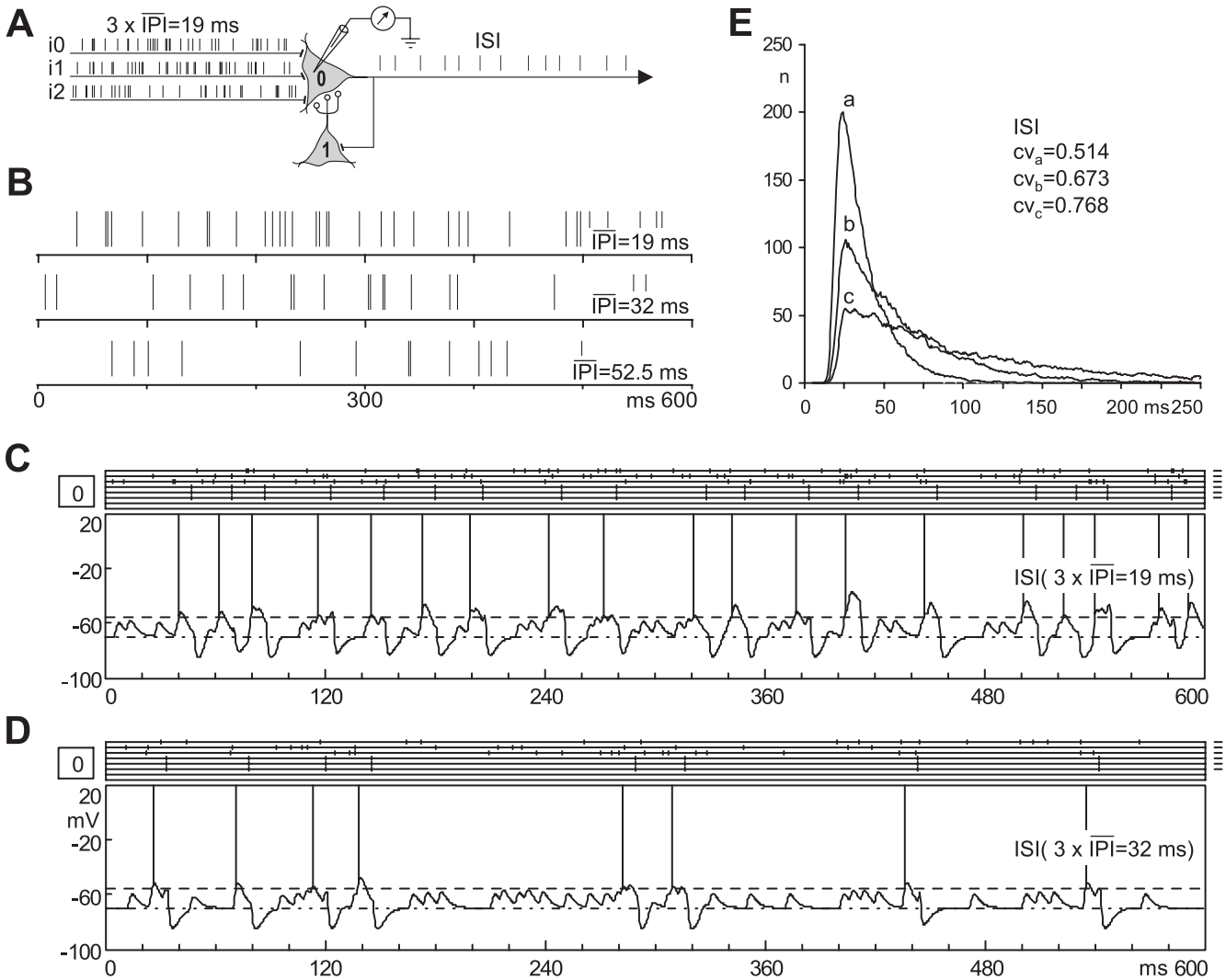

Fig. 2. A random excitatory afferentation balanced by a recurrent inhibition. A, a scheme of the integrating micronetwork (notation as in Fig. 1A). The stream of afferent signals was simulated by 3 independent Poisson distributed pulse trains with the same intensity (3 x $\overline{IPI}$ = 19 ms). The integrated output of the neuroid 0 was characterised by a variety of interspike intervals (ISI); B, a raster display of three samples of the Poisson distributed pulse trains with distinct intensities ($\overline{IPI}$ = 19 ms, 32 ms and 52.5 ms), spanning 600 ms period of the simulation time; C, representative spike train emitted by neuroid 0 during bombardment with independent Poisson distributed pulse trains arriving simultaneously via i0, i1 and i2. The intensity was the same in all three afferent pathways (3 x $\overline{IPI}$ = 19 ms). Other symbols, conventions and notation as in Fig. 1B; D, the same as in C with different intensity of the afferent pulse trains (3 x $\overline{IPI}$ = 32 ms); E, the histograms of interspike interval distribution. The occurrences of the intervals between adjacent spikes emitted by neuroid 0 was taken over 500 trails (each corresponding to 600 ms of simulation time) when receiving independent Poisson distributed pulse trains with three different intensities: 3 x $\overline{IPI}$ = 19 ms (**a**), 32 ms (**b**), 52.5 ms (**c**). The jitters in the ISI of output spikes were quantified by coefficient of variation (CV). Abscissa - ISI (using 2 ms bins), ordinate - number of events.

i2, 3 x $\overline{IPI}$ = 19 ms), and they were stochastically independent. Figs. 2C and D show typical spike trains emitted by neuroid 0 during bombardment with stochastic, Poisson distributed synaptic inputs: 3 x $\overline{IPI}$ = 19 ms (C) and 3 x $\overline{IPI}$ = 32 ms (D). Much variability in the microstructure of spiking was evident in each trial. The mean ISI taken over 500 trials (each corresponding to 600 ms of simulation time) equalled to 34.6 ms ($\overline{IPI}$= 19 ms), 57.2 ms ($\overline{IPI}$= 32 ms) and 85.9 ms ($\overline{IPI}$= 52.5 ms). The associated ISI histograms in Fig. 2E, a, b and c document a lack of very short intervals resulting from the recurrent inhibition and an exponentially decreasing

likelihood of finding very large gaps between consecutive spikes. The ISI variation in any spike train was less than the upper bound (1.0) given by a pure Poisson process: CV_{ISI} = 0.514 (a), 0.673 (b), 0.768 (c).

The input equipped with recurrent inhibition influenced the rate of both the excitatory and inhibitory drive, leading to a "random walk" of PSPs of the integrate-and-fire unit. The variation in the spiking of the neuroid 0 reflected the statistical properties of the input and the integration processes described above. The jitters in the timing of spikes (CV_{ISI} values) showed that in spite of the "massive" input the integrating neuroid preserved the capacity to transmit information in the rate-coding mode.

The key parameter of any integrate-and-fire model neurone, designed as a rate-encoding device, is the time interval during which it retains the information about its recent past. This is determined by the integration period (the time-course of the synaptic potentials) and the stimulus-evoked pre- and postsynaptic excitability cycles.

A time-course of the simulated postsynaptic potential produced in our neuroid is shown in Figs. 1B, D and E. With a monosynaptic excitatory drive (single spike, SW = 1.02 times threshold) an EPSP was set up 0.5 ms after the afferent spike (an arrow) had arrived at the presynaptic ending (Fig. 1D). The EPSP rose to a summit close to 2 ms after its origin. From the summit the EPSP declined with exponential time course, the time constant being 5.7 ms; the EPSP width measured at half-height was 5.5 ms. The falling phase lasted approximately 12 ms and the duration of the whole EPSP was roughly 14 ms. The spike-threshold depolarisation was 16 mV.

Figure 1E shows the responses of the neuroid with the above mentioned parameters to different modes of a subthreshold excitatory drive (SW = 0.5 times threshold). In the case of a 333 Hz input rate (a regular frequency, 3 ms ISI) the integration period compared with the ISI was longer, therefore the neuroid integrated EPSPs up to the spike threshold and the rate encoding came into effectiveness. At a 66 Hz input rate (ISI = 15 ms) there was no temporal summation - the EPSPs did not contribute to the generation of the spike potential. In this mode the neuroid failed to integrate the input - its capacity to participate in the rate coding was limited to high-rate inputs (a temporal summation of the activity).

It is evident that the rate encoding in the case of the lower spiking frequency is not possible without participation of some form of a memory. The reasonable possibilities are use-dependent pre- and/or postsynaptic plastic changes, which may have a distinct role in the integration of afferent signals (Gerstner et al. 1997).

A short-term facilitation: a mechanism that could be involved in rate encoding of the lower spiking frequency and in registering numerical quantities

One of the biologically relevant forms is a short-term synaptic enhancement known as paired-pulse facilitation, since it is observed after delivering a single pair of stimuli to a synapse. This homosynaptic mechanism depending on the history of the input activity has the presynaptic origin of its induction and lasts about 100 ms (Koch 1999).

Figure 3 shows the simulated responses of a neuroid, which received afferent signals *via* a plastic synapse (A, PS). The results showing the simulation of the paired-pulse stimulation protocol are in Fig. 3B, a-d. Different delays between conditioning stimulus (C) and each of the testing stimuli (T_1-T_4) were applied (10, 25, 40 and 55ms) (Fig. 3B, i0). The maximal facilitation in the EPSPs produced by the testing stimulus amounted to 211% (b, T_2) of the control (C). The enhanced synaptic transmission persisted for about 50 ms (c, T_3).

Synaptic transmission relies on the dynamics of the synaptic gain modified by strings of input spikes. The next simulation experiments illustrate the functioning of a plastic synapse (revealing the short-term facilitation), which was activated by strings of action potentials with a regular ISI (Fig. 3C, D). The presynaptic train of 4 spikes applied within a 57 ms window (53 Hz, ISI = 19 ms, the initial SW was equal to 0.14 times the threshold) induced the facilitation of the synaptic transmission manifested by 171% rise in the EPSP amplitude which exceeded the threshold (Fig. 3C, e, 3D, I). At the lower input rate (19 Hz, ISI = 52.5 ms) the dynamics of the synaptic gain changed. The spike-threshold level was exceeded after 7 input spikes arrived within a 315 ms window (Fig. 3C, f, 3D, II). After the count headed towards the spike-threshold level, a single testing input spike following the last spike in the train checked the persistence of the synaptic facilitation induced by a train of spikes. This measurement was repeated in several consecutive runs with a gradual prolongation of the time period between the last spike in the train and the testing spike. The decay time to the control level (Fig. 3E) was 103 ms for the 53 Hz train (I) and 48 ms for the 19 Hz train (II).

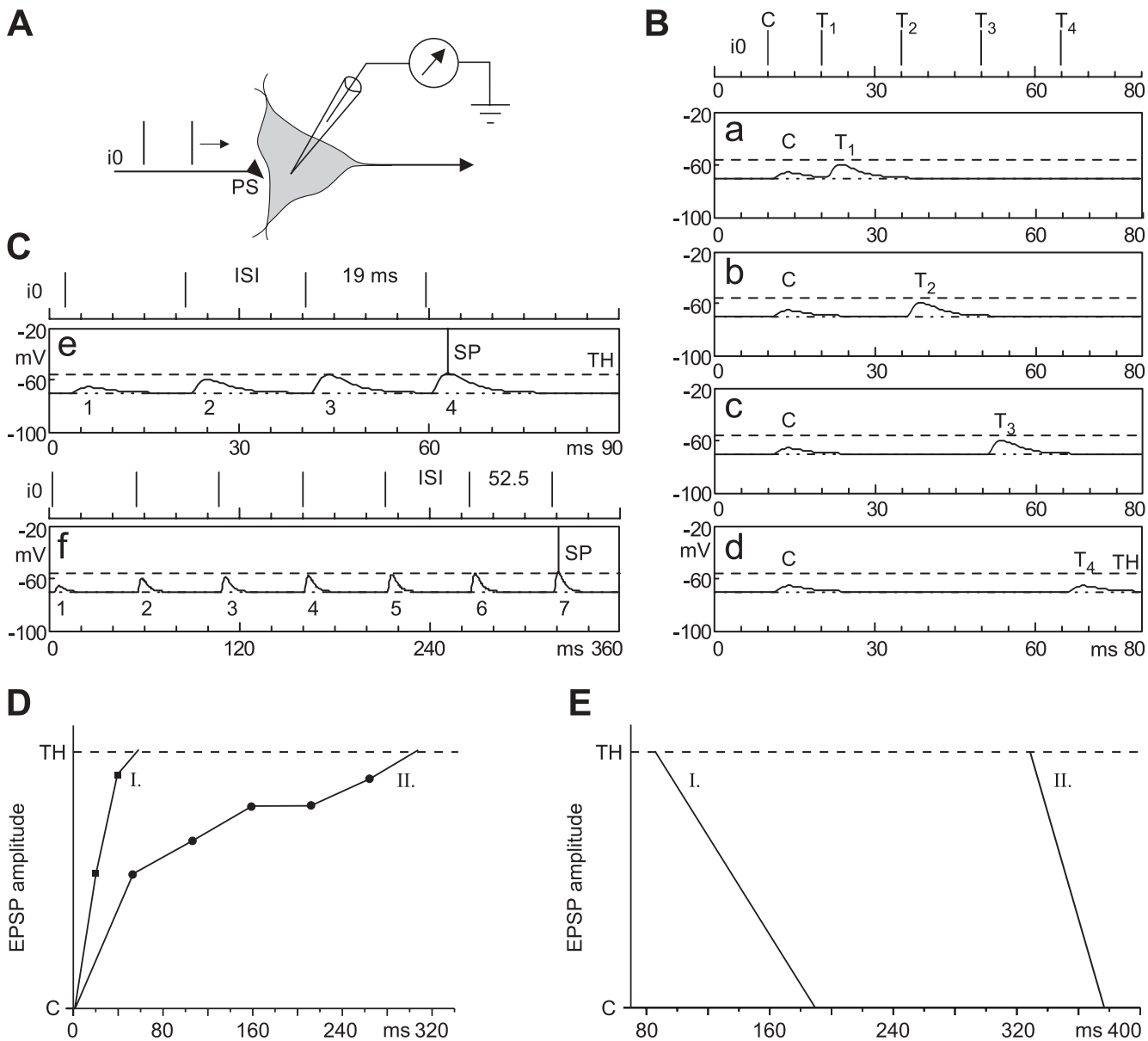

Fig. 3. The elementary quantitative abilities resulting from short-term presynaptic facilitation. A, neuroid excited with spikes transmitted in a single channel (i0) across a plastic synapse (PS); B, the paired-pulse stimulation protocol. The raster scheme in the upper part shows the temporal sequence of the input spikes. After the first - conditioning (C) stimulus followed the second - testing (T) stimulus with different delays ($T_1 - T_4$). Simulated pairs of the evoked excitatory postsynaptic potentials (EPSPs) are displayed in parts **a** – **d**. Other symbols, conventions and notation as in Fig. 1B; C, the facilitation of the synaptic gain of the PS induced by regular trains of action potentials with distinct interspike intervals (ISIs) (**e** - 19 ms, **f** – 52.5 ms). The EPSP exceeded the spike-threshold level after the fourth/seventh input spike (e, 4/f, 7). Other symbols and notation as in B, see text for details; D, the rise time of the EPSP amplitude from the control level (C = the amplitude of the first EPSP) to the spike-threshold level (TH) in the course of regular input spiking with ISI 19 ms (I) and 52.5 ms (II); E, decay time of the EPSP facilitation induced by a regular input spiking with ISI 19 ms (I) and 52.5 ms (II).

The results confirmed that the short-term presynaptic facilitation could be involved in integrative mechanisms enabling a rate encoding of the low rate spiking activity. At the same time it could serve as a "reservoir" of an analogous quantity estimating how numerous some events are. The increments of the accumulated quantity, represented by the enhancement of the synaptic efficiency, pushed the EPSP from its subthreshold

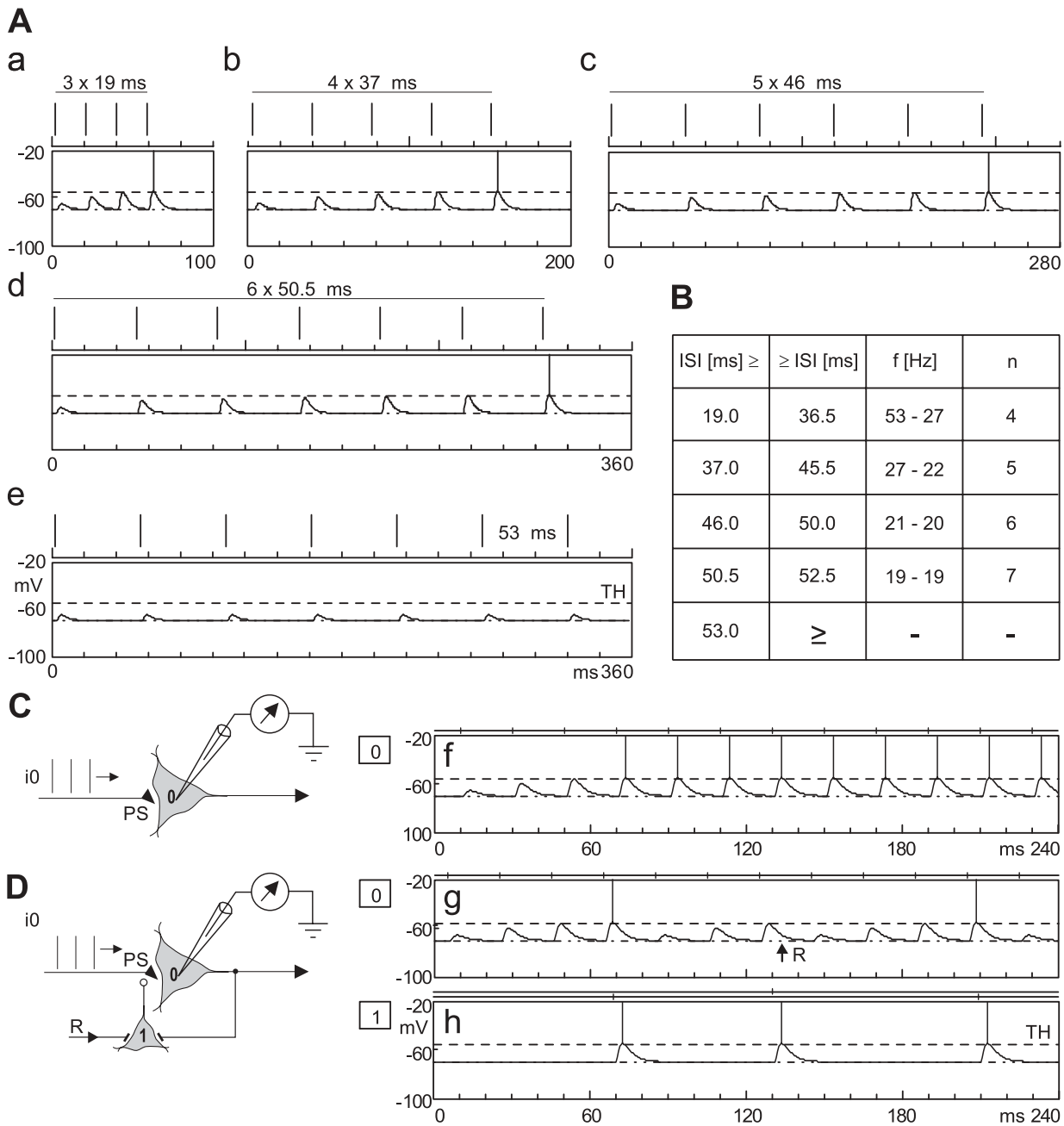

ISI [ms] ≥	≥ ISI [ms]	f [Hz]	n
19.0	36.5	53 - 27	4
37.0	45.5	27 - 22	5
46.0	50.0	21 - 20	6
50.5	52.5	19 - 19	7
53.0	≥	-	-

Fig. 4. Basic counting abilities. A, regular spike trains arriving at the plastic synapse (a raster display in upper parts of **a** - **d**) induced the facilitation of the synaptic gain. The amplitude increments of the simulated excitatory postsynaptic potential (lower parts of **a** - **d**) pushed its value to spike-threshold level. Other symbols and notation in a - e as in Fig. 1B. Depending on interspike interval (ISI, 19 - 52.5 ms range) the threshold was exceeded after a specific number of input signals - neuroid behaved as a counter of spikes: "number 4" (**a**), "number 5" (**b**), "number 6" (**c**) and "number 7" (**d**). The increase of the ISI length prolonged the counting period and enhanced the number of counted events (see also in B). When the ISI was longer than 52.5 ms (**e**) the short-term facilitation did not come into effectiveness and the counting of input spikes failed; B, lowering of the input rate narrowed the ISI range in which the number of counted events remained the same; C, continuous counting was impossible without a "reset" mechanism. If the regular train of input spikes (i0) transmitted across the plastic synapse (PS) continued after the spike-threshold level was reached, the neuroid 0 emitted spikes just copying the input frequency (**f**); D, a "reset" mechanism provided by an inhibitory neuroid (D, 1, h) that established an axo-axonic contact with PS of the neuroid 0. After each "reset" to "zero" the counting started from the control level (**g**). The "reset" could be evoked either via recurrent collateral (a loop 0-1-PS) or from other sources - R (D, g). Other symbols and notations in f - h are as in Fig. 1B.

level to the spike threshold and counting the number of stimuli seemed a relevant aspect of such behaviour.

The dynamics of the short-term presynaptic facilitation (Fig. 3B, C, D and E) showed that such a counter was not independent of the ISI length. The interspike intervals determined the time period over which the spikes were counted (Fig. 4). At higher input rates, the count tended towards the spike threshold before there was any time to decay. In the case of 19 ms ISI the neuroid behaved as "number 4" cell (the counting period was 3 x 19 ms = 57 ms) (Fig. 3C, e, Fig. 4A, a). In the case of 52.5 ms ISI the same neuroid behaved as "number 7" cell (the counting period was 6 x 52.5 ms = 315 ms) (Fig. 4A, d). In our simulation experiments with constant input rates numbers 4 and 7 represented lower and upper limits of counting (Fig. 4A, a - d, B, n).

The results showed that: a) the lowering of the input rate prolonged the counting period and increased the number of counted events. b) The lowering of the input rate narrowed the ISI range in which the number of counted events remained the same (Fig. 4B). c) The counting of input spikes failed when the ISI was longer than 52.5 ms (Fig. 4B). In this case the short-term facilitation did not come into effect and therefore the EPSP amplitude remained at the control level (Fig. 4A, e).

The counting process performed by any reservoir with a finite content presupposes the existence of some mechanism emptying the reservoir when it becomes full. In our simulation experiments this status corresponded to the situation when the EPSP reached the spike-threshold level (Fig. 4C, f). The neuroid 0 lost its counting ability - it emitted a spike at each successive stimulus in the sequence with the frequency just matching the input rate. The solution to this problem was a hypothetical "reset" mechanism carried out by a modulatory neuroid establishing an axo-axonic synapse with presynaptic terminals (Fig. 4D, neuroid 1). Its spiking (Fig. 4D, h) should rapidly and reversibly cancel the facilitation of the plastic synapse. Such a "reset" effect can be evoked either *via* recurrent collateral (a feedback control - Fig. 4D, neuroids 0 - 1) or from other sources (Fig. 4D, afferent R). After each "reset" to "zero" the counting started from the control level (Fig. 4D, g).

Natural stimuli elicit a changeable number of action potentials and the time between successive spikes (ISI) can show a marked variation. The integration of synaptic inputs over space and time should act as a basis for counting irrespective of regularity or randomness of the input spikes. In the following simulation experiments the performance of a devised counting mechanism was tested under conditions of irregular spike trains.

The fact that the counting period is not independent of the ISI length prompted us to analyse the influence of different sequential ordering of unequal ISIs, all belonging to one of the ISI ranges, in which the neuroid

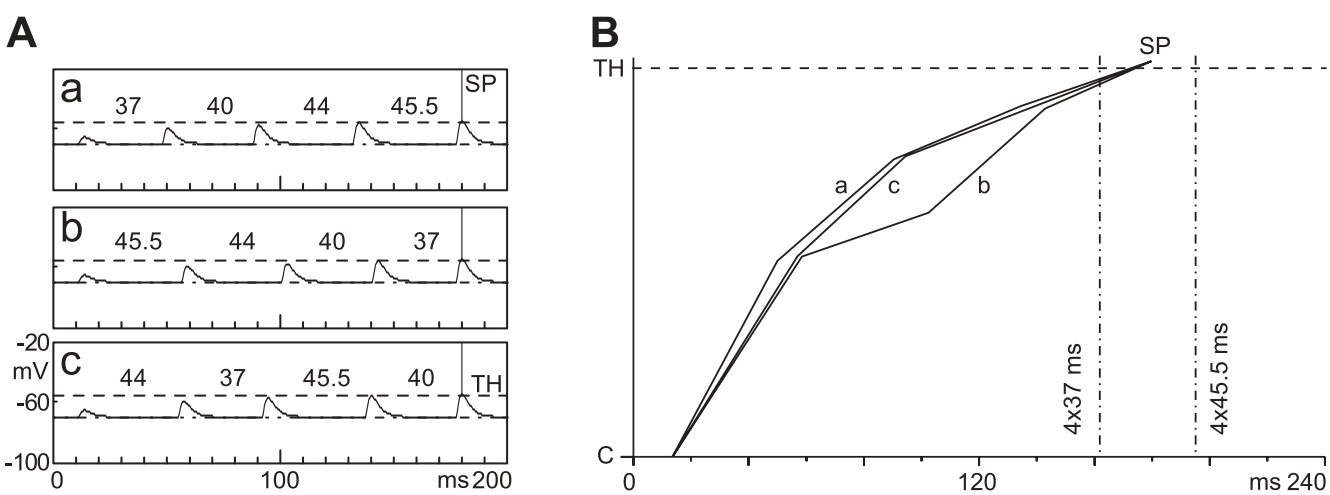

Fig. 5. Counting of spikes in irregular spike trains. A, simulated excitatory postsynaptic potentials (EPSPs) in a neuroid excited by a train of five spikes transmitted across a plastic synapse. All interspike intervals - ISIs (37, 40, 44 and 45.5 ms) in each train (**a**, **b** and **c**) belonged to the ISI range, in which the neuroid behaved as a "number 5" unit (see Fig. 4B). Regardless of a distinct sequential ISI ordering the output spike (SP) was emitted in all cases in the 180th ms of the simulation time. Other symbols and notation in a - c as in Fig. 1B; B, changes of the ISIs sequence shown in part A caused differences in increments of the EPSP amplitudes evoked by consecutive input spikes (curves **a**, **b** and **c**). The point of intersection of all three curves at the spike-threshold level (TH) corresponded to the 180th ms of the simulation time. Two vertical dash-dot lines indicate the time interval within which the neuroid behaved as a "number 5" unit. Abscissa - simulation time, ordinate - EPSP amplitude (C - control).

behaved as a counter sensing a single number. Fig. 5A shows the responses of the "number 5" neuroid (the ISI range 37 - 45.5 ms - Fig. 4B). Changes in the ordering of four distinct ISIs (37, 40, 44 and 45.5 ms) (Fig. 5A, a - c) caused differences in increments of the EPSP amplitudes evoked by individual input spikes (Fig. 5B, a - c). The unequal time courses of the EPSP increments resulted from the integration of two counter-acting processes: the short-term facilitation (analogous to an inflow into a reservoir) and the duration of the quiet periods (an outflow). The information about the exact input spike times was "forgotten" because in all cases the output spike was emitted in the 180th ms of the simulation time, without regard to the sequential ordering of the ISI (Fig. 5A, a, b and c, B). It means that the devised counter behaved as a mean-rate decoder - the presynaptic inputs determined the average rate of postsynaptic discharges, but the temporal patterns (ordering of intervals) did not convey information.

A network performing the discrimination of the rate-encoded inputs

In the next section we present a neural model devised for continual comparison of the spike trains entering the network simultaneously along parallel channels, containing a mixture of interspike intervals of different lengths. The network should show the difference in the mean spiking rates between the channels.

MAIN FUNCTIONAL BLOCKS

As is shown on the schema-level model (Fig. 6A) the network was composed of two parallel channels (1, 2). The inputs into the channels were represented by independent pulse trains (arrows) simulating an afferentation from distinct receptor areas. Each channel consisted of three functional blocks: a) integrator at the input (INTGR). b) Counter (CNTR). c) A gated output (GATE). The activity flow is indicated by black arrowheads, the white arrowheads show mutual functional contacts between blocks belonging to distinct channels.

NETWORK STRUCTURE

A "neuronal" circuitry hidden in the "black boxes" of the schema-level model is shown in Fig. 6B. The network consisted of 10 neuroids (0-9). Three afferents established monosynaptic connections with the input neuroid 0 (i0-i2, channel 1) and 6 (i3-i5, channel 2). The suprathreshold excitatory responses of the neuroids 0 and 6 were controlled by a recurrent postsynaptic inhibition mediated *via* neuroids 1 (a loop 0-1-0) and 7 (a loop 6-7-6). The neuroid 0/6 formed monosynaptic connection with neuroid 2/8; those functional contacts had characteristics of the plastic synapse described above (Fig. 3). The neuroids 2 and 8 had divergent projections - each of them to three other units. They established convergent excitatory connections with the neuroids 4 and 5; the third axonal branch of the neuroid 2/8 made synapse with the output neuroid 3/9 (channel 1/channel 2). The divergent projections of the neuroid 4 and 5 mediated mutual functional influences between channel 1 and 2. The neuroid 4 formed recurrent axo-axonal (presynaptic) inhibitory connections with plastic synapses attached to neuroids 2 and 8, and the neuroid 5 generated a postsynaptic inhibition of the output units in the channel 1(neuroid 3) and 2 (neuroid 9).

NETWORK PARAMETERS AND ACTIVITY FLOW

The neuroids 0 and 6 integrated their irregular inputs (Poisson processes) temporally as well as spatially; each arriving spike depolarised the neuroid 0/6 by 73% of the spike-threshold level (see Fig. 1B). The dynamic range of their spiking was predetermined to 100 - 350 spikes/s as limits for slightly suprathreshold and maximal depolarisation. The integration of many uncorrelated, random EPSPs was balanced by the recurrent inhibition - a single spike emitted by the neuroid 1/7 induced the hyperpolarization of the neuroid 0/6 amounting to 21% of the resting membrane potential. The model with the indicated parameters provided considerable variation in both the timing of spikes (ISIs) and their counts (Fig. 6C, neuroids 0 and 6). The responses of the neuroid 0/6 were "decoded" by neuroid 2/8 (Fig. 6B) that counted their spikes by means of mechanisms described above (Figs. 4 and 5). When the count exceeded a threshold barrier, either in the neuroid 2 or 8, "the winner's" spike excited with the suprathreshold intensity the neuroid 4, which abolished the presynaptic facilitation at the level of plastic synapses in both channels. Thus "the winner" "resetted" the count to "zero" and the counting started again from the initial level. Fig. 6C and D show the responses of the neuroids 0, 2, 4, 6 and 8 under condition of different input rates to the channel 1 (3 x $\overline{IPI}$ = 19 ms) and channel 2 (3 x $\overline{IPI}$ = 32 ms). In this simulation experiment the neuroid 2 (compared with the neuroid 8) "won" 4:0; its spikes were conveyed to the

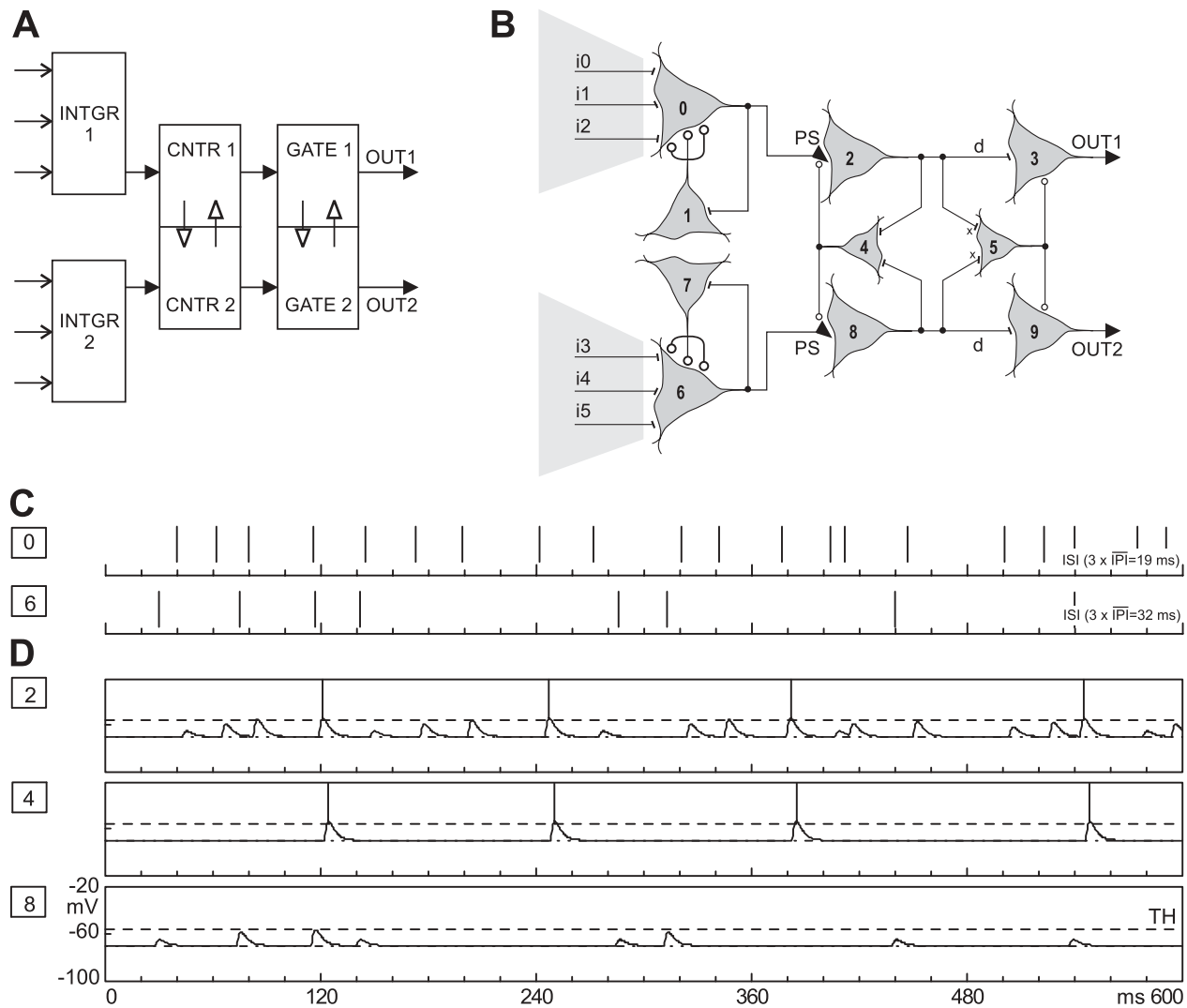

Fig. 6. Neural network performing detection of the mean spiking rate difference between irregular spike trains propagated along two parallel channels. A, schema-level model. Both channels (1, 2) were composed of three functional blocks: An integrator (INTGR), a counter (CNTR) and a gated output (GATE). Arrows - the input, black arrowheads - the activity flow, white arrowheads indicate mutual functional contacts between blocks belonging to distinct channels; B, a network architecture. A triad of independent parallel afferents (i0 -i2 and i3 - i5) simulated each of two distinct inputs into the network from imaginary receptor areas (grey fields). Functional connections among ten neuroids (0-9) marked by bars are excitatory. Circles denote synapses evoking postsynaptic inhibition (5 - 3 and 5 - 9) and a tentative presynaptic disfacilitation (4 - 2 and 4 - 8). Crosses indicate subthreshold excitatory influence, d indicates a delay line. PS - activity-dependent plastic synapses; C, a raster display of spiking activity of the integrating units (neuroid 0 - channel 1, neuroid 6 - channel 2) evoked by streams of irregular afferent signals with different intensities (3 x $\overline{IPI}$ = 19 ms for channel 1 and 3 x $\overline{IPI}$ = 32 ms for channel 2); D, simulated postsynaptic responses of neuroids 2, 4 and 8 forming the counters. The higher mean spiking rate of the train entering the channel 1 was signalled by discharge activity of neuroid 2. See text for details. The other symbols and notation as in Fig. 1B.

output unit (the neuroid 3) belonging to the same channel (1). The propagated responses of the neuroid 2 (Fig. 6D, 2) and consequently those of the neuroid 3 (not shown) demonstrated two facts: a) in the course of 600 ms of the simulation time the mean spiking rates in the channel 1 and 2 were unequal, b) the network made a decision in which channel was the mean spiking rate higher.

If there was no difference in compared mean spiking rates, the "competing" counters (the neuroids 2 and 8) emitted spikes at the same moments. As the mean spiking rates were the same, the outputs of the channel 1

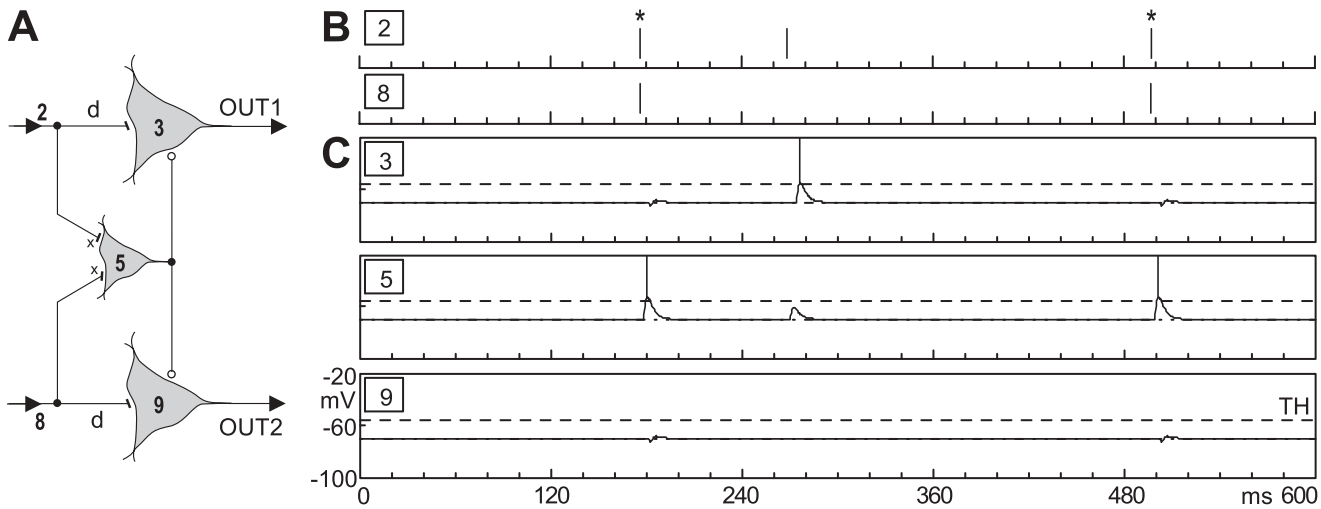

Fig. 7. "Gating" mechanism. A, a circuitry forming a "gated" output (neuroids 3, 5 and 9) of the network illustrated on Fig. 6B. Functional connections marked by bars (circles) are excitatory (inhibitory). Crosses indicate subthreshold excitatory influence, d indicates a delay line; B, a raster display simulates spiking activity in 2 and 8 entering the "gated" output; C, simulated postsynaptic responses of neuroids 3, 5 and 9. A temporal coincidence of spikes arriving along 2 and 8 (asterisks) caused the inhibitory neuroid 5 to fire a propagated action potential that inhibited responses of the neuroids 3 and 9 forming the outputs of the network. See text for details. Other symbols and notation are as in Fig. 1B.

(neuroid 3) and channel 2 (neuroid 9) should have remained silent. This effect was achieved by means of the implemented "gating" mechanism illustrated in Fig. 6B and 7A. The structural constituent, of the "gating" was: a) one inhibitory neuroid (5) supplied with a synaptic input formed by collaterals branched off from axons of the neuroids 2 and 8 (convergence), b) divergent projection of the neuroid 5 to the neuroids 3 and 9. The main functional principles involved in the "gating" were: a) a conduction delay (d = 4 ms) between the counters (the neuroids 2 and 8) and the output units (neuroids 3 and 9), b) a subthreshold excitatory influence of the neuroid 2 and 8 on the neuroid 5 (denoted with crosses), c) because of subthreshold excitation of the neuroid 5, the propagated spike in its axon was set up (Fig. 7C, neuroid 5) only when a temporal coincidence of spikes arriving to the neuroid 5 occurred (Fig. 7B, neuroids 2 and 8) and a maximal spatio-temporal summation of their excitatory influences was induced, d) the efferent discharge of the neuroid 5 (a coincidence detection) caused a feed-forward postsynaptic inhibition of both output neuroids (3 and 9) that prevented their firing (Fig. 7C, neuroids 3 and 9).

DETECTABLE RATE DIFFERENCES

Our next task was to determine whether the proposed scheme was sufficiently sensitive to distinguish different spiking rates. In our model, all spike trains form finite-time samples of stochastic processes. Hence, the theoretical intensities of the processes can not be compared with absolute certainty. From the statistical point of view, the best method is to base the comparison on counts, i.e. the number of spikes in each sample. Therefore, we calculated the probabilities that the comparison of counts at the level of input (neuroids 0 and 6) and at the level of output (neuroids 3 and 9) leads to the correct judgement which intensity is greater. In this way it was possible to evaluate the ability of the network to differentiate distinct intensities (sensitivity) and the extent to which the processed information was preserved.

Let us suppose that the input into channel 1 represents the ideal Poisson process with mean interspike intervals $\overline{IPI}$ 1, and the input into channel 2 represents the ideal Poisson process with mean interspike intervals $\overline{IPI}$ 2. Let the symbols $N1_{Id}(\overline{IPI}\ 1)$ and $N1_{Id}(\overline{IPI}\ 2)$ denote the random number of spikes at the input of channel 1 (neuroid 0) and channel 2 (neuroid 9) within the 600 ms period. The random number of spikes at the output of channel 1 (neuroid 3), and channel 2 (neuroid 9) depends on both $\overline{IPI}$ 1 and $\overline{IPI}$ 2. This fact results from mutual functional contacts between both channels. Therefore we denoted the number of spikes at the outputs by $N1(\overline{IPI}\ 1, \overline{IPI}\ 2)$ for channel 1, and $N2(\overline{IPI}\ 1, \overline{IPI}\ 2)$ for channel 2.

We used simulations with different combinations of $\overline{IPI}$ 1 and $\overline{IPI}$ 2, to estimate the probability that the num-

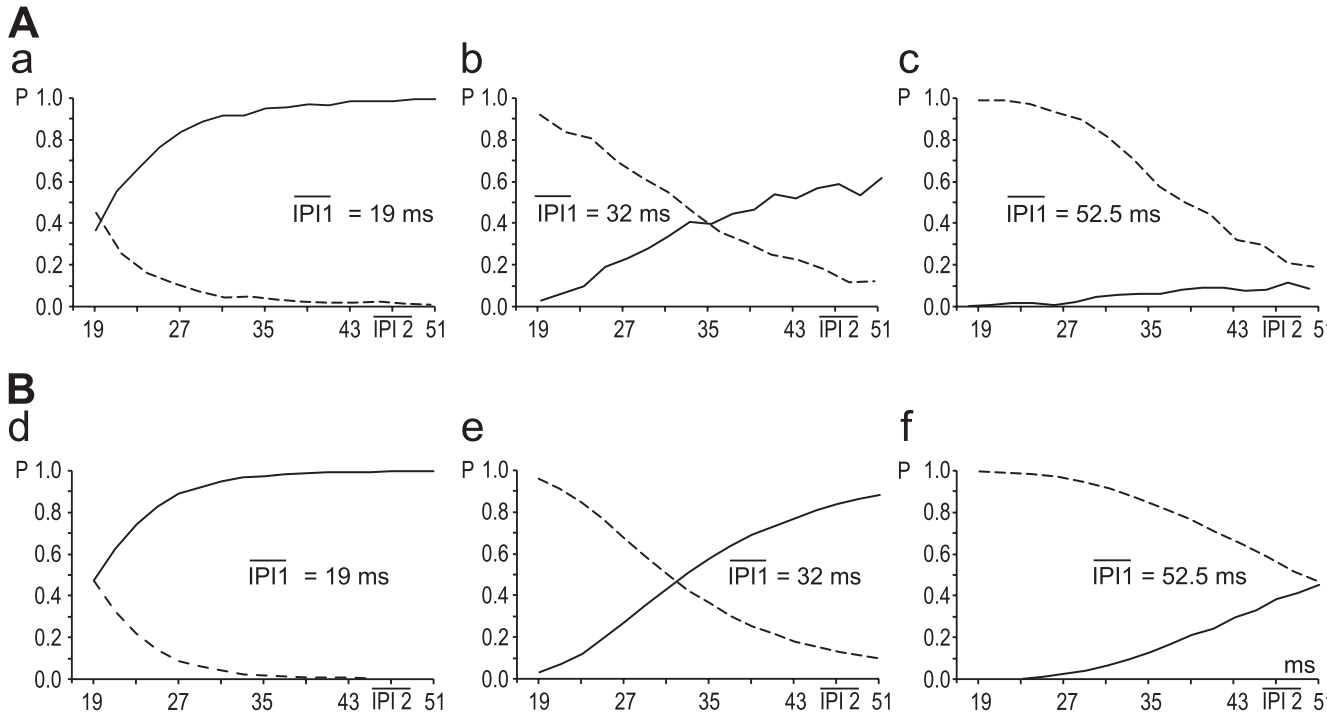

Fig. 8. Exactness of the mean-rate discrimination. A, probabilistic comparison of information about the difference in intensities of the Poisson distributed pulse trains entering the network within a 600 ms simulation period at the level of the output neuroids 3 and 9 (Fig. 6B). In **a**, **b**, and **c** are plotted probabilities of winnings (solid lines) and losses (dashed lines) of inputs with intensities $\overline{IPI}$ 1 = 19 ms, 32 ms and 52.5 ms against the selected spectrum of intensities in the 19 - 51 ms range ($\overline{IPI}$ 2, 2 ms bin). The winning and the loss is based on the number of spikes at the level of the output neuroids 3 and 9. Each $\overline{IPI}$ 1 was simulated by integration of 3 independent Poisson distributed pulse trains with the same intensity (Fig. 2A). The curves which represent the dynamics of the probability prediction were obtained from 500 simulation runs for each combination of $\overline{IPI}$ 1, $\overline{IPI}$ 2; B, same as A, but the winning and the loss was determined by the number of counting events associated with an ideal Poisson process (see text for details). The curves of the probability prediction were obtained from 10,000 simulation runs for each combination of $\overline{IPI}$ 1, $\overline{IPI}$ 2.

ber of output spikes in channel 1 is greater (or less) than the number of output spikes in channel 2. In Fig. 8A,$\overline{IPI}$ 1 was set to 19 ms (a), 32 ms (b) and 52.5 ms (c), while $\overline{IPI}$ 2 increased in the range from 19 ms to 51 ms in 2 ms steps (the same holds for part B). For each combination, the estimate was based on 500 simulation runs. For example, when comparing $\overline{IPI}$ 1=19 ms with $\overline{IPI}$ 2=27 ms we can estimate with probability 0.83 that the number of output spikes from channel 1 is greater than that from channel 2 (Fig. 8A, a).

The probabilities at the output of the network (Fig. 8A) were compared with the probabilities at the input (Fig. 8B). The number of input spikes to channel 1 ($N1_{Id}(\overline{IPI}\ 1)$) and to channel 2 ($N2_{Id}(\overline{IPI}\ 2)$), and the probabilities at the level of inputs were calculated from 10,000 simulation runs. Using the same example as mentioned above (the comparison of $\overline{IPI}$ 1=19 ms with $\overline{IPI}$ 2=27 ms) we obtained probability 0.89 that the number of spikes arriving at the input of the channel 1 was grater. The small difference between probabilities revealed that for a short $\overline{IPI}$ 1 (19 ms), the loss of relevant information was very low (graphs A, a and B, d). It became more evident with $\overline{IPI}$ 1 increase (graphs A, c and B, f). This fact was mainly due to the larger proportion of the "gated" outputs.

The analysis of the network capacity to distinguish the different spiking rates revealed that the same generic results were obtained with only little reduction of information compared to the probability of theoretically best comparison.

DISCUSSION

Continuous monitoring and comparison of spike frequencies originating from vast, simultaneously activated receptor areas is an unavoidable condition for

sensory processing. It is the relative firing of the different neurones that provides the information about distinct events. To utilise the rate code, mechanisms able to detect the differences between firing rates in individual sensory channels have to be assumed (Pavlásek and Hromádka 2001). This idea is connected with the following problems: a) an optimal integration of multiple inputs, b) counting of spikes by means of biophysically relevant mechanisms, c) a neurobiologically plausible architecture and computational logic of the neural network.

A temporal structure of spike trains carrying information about stimulus features results mainly from the integration of postsynaptic currents in the dendritic trees (Segev and London 2000, Shepherd 1996) of "early" and "upstream" neurones in relay nuclei of sensory pathways. Independent and irregular spike trains conveyed in large number of afferents represent the responsible inputs. Therefore the key point valid for any integration unit is its ability to accommodate a large number of inputs (a "data compression") and at the same time maintain the appropriate dynamic range of the output spiking in order to preserve temporal accuracy with changes in the stimulus. Considering the intrinsic neuronal processes, the variation in the ISI depends on a "random walk" of the membrane potential shifts (Gerstein and Mandelbrot 1964) between the resting potential and the spike threshold level. With roughly equal amounts of excitation and inhibition, the ISI can be highly irregular (Calvin and Stevens 1968). To achieve this status with a plausible neurophysiological implementation, a negative feedback, provided by the recurrent inhibition, represents a reliable mechanism. A match between the mean-rate distinction expressed as a probability of the theoretically best comparison (Fig. 8B, d, e and f) and the results achieved by a devised network (Fig. 8A, a, b and c) suggests that the microcircuit provided minimal degeneration of the information concerning the intensity of the input spike trains.

Postsynaptic neurones are able to perform more complicated tasks than computing the weighted average of their inputs. We have shown that the neuroid can decipher the rate-encoded stimulus by counting the spikes.

In an earlier work Thompson et al. (1970) called attention to the fact that higher mammals appear able to abstract number of events. The responses of the observed neurones were at least to some degree independent of particular stimulus characteristics. These results were in concert with a view that more abstract aspects of perception may be represented by single neurones termed gnostic cells (Konorski 1967). Some inspiring ideas about numerical perception (a "numerosity" sensing) were connected with the concept of a "mental module" functioning as an "accumulator" that could hold a register of various quantities (Dehaene 1997). This model makes it possible to estimate how numerous some events are, but does not enable us to compute their exact number.

The computational implications of rapid forms of plasticity have not received much attention and cerebral circuits for events counting remain largely unknown. Some authors interpreted the short-term synaptic enhancement as a "burst filter" that increases the probability of successful transsynaptic signal transmission (Koch 1999). We used the simulation of the short-term presynaptic facilitation to increase the network capabilities to retain the information about the time course of events within the irregular, low-rate spike train (the ISI range 19 - 52.5 ms). Depending on the sum of the successive ISI lengths in the train (without respect to their ordering) the integration unit typically responded to a particular input spike in the sequence. In our simulation experiments the number-detecting neuroid coded the concept of numbers 4, 5, 6, and 7. This is in agreement with the counting cells observed in association with the cortical areas of the cat that coded the numbers 2, 5, 6, and 7 (Thompson et al. 1970).

The crucial question in counting based on the accumulation of some quantity (the presynaptic facilitation in this case) is the possibility of its prompt removal after it attained certain levels (the threshold). The cellular and molecular processes underlying presynaptic modulation remain largely undetermined because of the difficulties in manipulating and recording from presynaptic terminals. It is reasonable to suppose that the ionotropic receptors are involved in short-term plastic changes (Traub et al. 1999) and possibly in their rapid extinction. The activity-dependent rise of free calcium content in presynaptic terminals (Kandel 1981, Koch 1999) could be the crucial signal triggering the EPSP amplitude increase when paired-pulse stimulation is applied (a homosynaptic mechanism). Such facilitatory effect might be overridden by ionic fluxes through ligand-gated channels with fast kinetics, tending to inactivate calcium transients and restore the resting electrochemical gradients in synaptic endings (a heterosynaptic disfacilitation). In this context presynaptic ionotropic AMPA/kainate receptors and a "shunting" inhibition could be mentioned (Koch 1985).

The model networks, application of information theory and procedures of mathematical statistics provide an important contribution to solving questions connected with neural coding (Borst and Theunissen 1999). Their value for neurobiology depends on whether the results achieved could be implemented by plausible neural circuits and biophysically reasonable mechanisms (Bialek et al. 1991, Bullock 1997, Perkel and Bullock 1968).

The "reading" of the rate code by postsynaptic neurones is essentially the problem of a network that operates continuously on the spike train to produce a real-time estimate of an unknown event. The main task is to distinguish, recognise and categorise the stimulus.

The architecture of the devised network (e.g., convergence, divergence, axo-somatic and axo-axonic synapses) and the functional mechanisms involved (e.g., parallel processing, spatio-temporal summation of postsynaptic potentials, plastic synaptic changes, feedback and feed-forward inhibition, coincidence detection, delay lines, gating) are so widespread in the central nervous system that it is sound to consider their potential use at any level of information processing. It would be interesting to verify by neurophysiological and psychophysiological experiments to what extent the results reported here could be of behavioural significance. Such trajectory might be productive both in terms generating interesting questions and in terms proposing answers.

ACKNOWLEDGMENTS

Slovak Grant Agency VEGA (grant No. 2/1011/22) supported this work, in part.

Thanks are due to Mr. Branislav Abel for his valuable technical help and to Mr. Nicholas P. Lee who has assisted by correcting English where necessary.

REFERENCES

Abbot L., Sejnowski T.J. (Editors) (1999) Neural codes and distributed representations. A Bradford Book, The MIT Press, Cambridge, Massachusetts, London, England, 345 p.

Adrian E.D., Zotterman Y. (1926) The impulses produced by sensory nerve-endings. Part 2. The response of a single end-organ. J Physiol (London) 61: 151-171.

Bialek W., Rieke F., deRuyter vanStevenick R.R., Warland D. (1991) Reading a neural code. Science 252: 1854-1857.

Borst A., Theunissen F.E. (1999) Information theory and neural coding. Nature Neuroscience 2: 947-957.

Bullock T.H. (1997) Signals and signs in the nervous system: The dynamic anatomy of electrical activity is probably information-rich. Proc Natl Acad Sci USA 94: 1-6.

Calvin W., Stevens C. (1968) Synaptic noise and other sources of randomness in motoneuron interspike intervals. J Neurophysiol 31: 574-587.

Cox D.R., Smith W.L. (1954) On the superposition of renewal processes. Biometrika 41: 91-99.

Dehaene S. (1997) The number sense. How the mind creates mathematics. Oxford University Press, 274 p.

deCharms R.D., Zador A. (2000) Neural representation and the cortical code. Annu Rev Neurosci 23: 613-647.

Gerstein G., Mandelbrot B. (1964) Random walk models for the spike activity of single neurons. Biophys J 4: 41-68.

Gerstner W., Kreiter A.K., Markram H., Herz A.V.M. (1997) Neural codes: firing rates and beyond. Proc Natl Acad Sci USA 94: 12740-12741.

Girman S.V., Sauvé Y., Lund R.D. (1999) Receptive field properties of single neurons in rat primary visual cortex. J Neurophysiol 82: 301-311.

Hsiao S.S., Johnson K.O., Twombly I.A. (1993) Roughness coding in the somatosensory system. Acta Psychol 84: 53-67.

Jančo J., Stavrovský I., Pavlásek J. (1994) Modeling of neuronal functions: A neuronlike element with the graded response. Comput Artif Intellig 13: 603-620.

Kandel E.R. (1981) Calcium and control of synaptic strength by learning. Nature 293: 697-700.

Koch C. (1985) Understanding the intrinsic circuitry of the cat's lateral geniculate nucleus: Electrical properties of the spine-triad arrangement. Proc Roy Soc Lond B 225: 365-390.

Koch C. (1999) Biophysics of computation. Oxford Univ. Press, New York, Oxford, 562 p.

Konishi M. (1991) Similar algorithms in different sensory systems and animals. In: The brain, Vol. LV of cold spring harbor symposia on quantitative biology. Cold Spring Harbor Laboratory Press, New York, p. 575-584.

Konorski J. (1967) Integrative activity of the brain: An interdisciplinary approach. Univ. of Chicago Press, Chicago.

König P., Engel A.K., Singer W. (1996) Integrator or coincidence detector? The role of the cortical neuron revisited. Trends Neurosci 19: 130-137.

Mountcastle V.B. (1957) Modality and topographic properties of single neurons of cat's somatosensory cortex. J Neurophysiol 20: 408-434.

Nádasdy Z. (2000) Spike sequencies and their consequences. J Physiol (Paris) 94: 505-524.

Pavlásek J., Hromádka T. (2001) Neural network comparing two rate-encoded inputs entering in parallel. Gen Physiol Biophys 20: 61-82.

Pavlásek J., Jenča J. (2001) Temporal coding and recognition of uncued temporal patterns in neuronal spike trains: biologically plausible network of coincidence detectors and coordinated time delays. Biologia 56: 591-604.

Perkel D.H., Bullock T.H. (1968) Neural coding. Neurosciences Res Prog Bull 6: 221-348.

Platt M.L., Glimcher P.W. (1999) Neural correlates of decision variables in parietal cortex. Nature 400: 233-238.

Redman S., Walmsley B. (1983) The time course of synaptic potentials evoked in cat spinal motoneurones at identified group Ia synapses. J Physiol (London) 343: 117-133.

Rieke F., Warland D., de Ruyter van Steveninck R., Bialek W. (1999) Spikes. Exploring the neuronal code. A Bradford Book, The MIT Press, Cambridge, Massachusetts, London, England, 395 p.

Segev I., London M. (2000) Untangling dendrites with quantitative models. Science 290: 744-750.

Segundo J.P., Perkel D.H., Wyman H., Hegstad H., Moore G.P. (1968) Input-output relations in computer-simulated nerve cells. Influence of the statistical properties, strength, number and inter-dependence of excitatory pre-synaptic terminals. Kybernetik 4: 157-171.

Shadlen M.N., Newsome W.T. (1994) Noise, neural codes and cortical organization. Curr Opin Neurol 4: 569-579.

Shepherd G.M. (1996) The dendritic spine: A multifunctional integrative unit. J Neurophysiol 75: 2197-2210.

Theunissen F., Miller J.P. (1995) Temporal encoding in nervous systems: A rigorous definition. J Computational Neurosci 2: 149-162.

Thompson R.F., Mayers K.S., Robertson R.T., Patterson Ch.J. (1970) Number coding in association cortex of the cat. Science 168: 271-273.

Towee M., Rolls E., Bellis R. (1993) Information encoding and the responses of single neurons in the primate visual cortex. J Neurophysiol 70: 640-654.

Traub R.D., Jefferys J.G.R., Miles A. (1999) Fast oscillation in cortical circuits. A Bradford Book, The MIT Press, Cambridge, Massachusetts, and London, 324 p.

Willis W.D. Jr., Coggeshall R.E. (1991) Sensory mechanisms of the spinal cord. Plenum Press, New York, 575 p.

Xu Z.C., Pulsinelli W.A. (1996) Electrophysiological changes of CA1 pyramidal neurons following transient forebrain ischemia: an *in vivo* intracellular recording and staining study. J Neurophysiol 76: 1689-1697.

Received 20 August 2002, accepted 24 April 2003